A LETTERS JOURNAL EXPLORING THE FRONTIERS OF PHYSICS

OFFPRINT

Impact of CNT medium on the interaction between ferromagnetic nanoparticles

A. L. Danilyuk, I. V. Komissarov, A. V. Kukharev, F. Le Normand, J. M. Hernandez, J. Tejada and S. L. Prischepa

EPL, **117** (2017) 27007

epl

A Letters Journal Exploring the Frontiers of Physics

AN INVITATION TO SUBMIT YOUR WORK

epljournal.org

The Editorial Board invites you to submit your letters to EPL

EPL is a leading international journal publishing original, innovative Letters in all areas of physics, ranging from condensed matter topics and interdisciplinary research to astrophysics, geophysics, plasma and fusion sciences, including those with application potential.

The high profile of the journal combined with the excellent scientific quality of the articles ensures that EPL is an essential resource for its worldwide audience. EPL offers authors global visibility and a great opportunity to share their work with others across the whole of the physics community.

Run by active scientists, for scientists

EPL is reviewed by scientists for scientists, to serve and support the international scientific community. The Editorial Board is a team of active research scientists with an expert understanding of the needs of both authors and researchers.

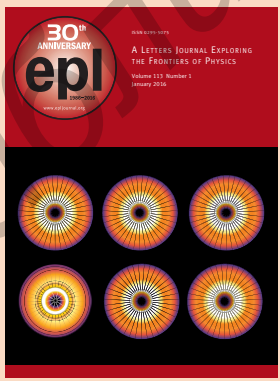

OVER
568,000
full text downloads in 2015

18 DAYS
average accept to online publication in 2015

20,300
citations in 2015

"We greatly appreciate the efficient, professional and rapid processing of our paper by your team."

Cong Lin
Shanghai University

Six good reasons to publish with EPL

We want to work with you to gain recognition for your research through worldwide visibility and high citations. As an EPL author, you will benefit from:

1. **Quality** – The 60+ Co-editors, who are experts in their field, oversee the entire peer-review process, from selection of the referees to making all final acceptance decisions.
2. **Convenience** – Easy to access compilations of recent articles in specific narrow fields available on the website.
3. **Speed of processing** – We aim to provide you with a quick and efficient service; the median time from submission to online publication is under 100 days.
4. **High visibility** – Strong promotion and visibility through material available at over 300 events annually, distributed via e-mail, and targeted mailshot newsletters.
5. **International reach** – Over 3200 institutions have access to EPL, enabling your work to be read by your peers in 100 countries.
6. **Open access** – Articles are offered open access for a one-off author payment; green open access on all others with a 12-month embargo.

Details on preparing, submitting and tracking the progress of your manuscript from submission to acceptance are available on the EPL submission website **epletters.net**.

If you would like further information about our author service or EPL in general, please visit **epljournal.org** or e-mail us at **info@epljournal.org**.

EPL is published in partnership with:

European Physical Society | Società Italiana di Fisica | EDP Sciences | IOP Publishing

A Letters Journal Exploring the Frontiers of Physics

January 2017

EPL, **117** (2017) 27007
doi: 10.1209/0295-5075/117/27007

www.epljournal.org

Impact of CNT medium on the interaction between ferromagnetic nanoparticles

A. L. Danilyuk[1], I. V. Komissarov[1,2], A. V. Kukharev[1], F. Le Normand[3], J. M. Hernandez[4], J. Tejada[4] and S. L. Prischepa[1,2]

[1] *Belarusian State University of Informatics and Radioelectronics - P. Browka 6, Minsk 220013, Belarus*
[2] *National Research Nuclear University "MEPHI" - Kashirskoe Highway 31, Moscow 115409, Russia*
[3] *Laboratory of Engineering, Informatics and Imagery (ICube) - Départment Electronique des Solides, des Systèmes et de Photonique (DESSP), Université de Strasbourg and CNRS - Bat. 28, 23 Rue du Loess, BP 20 CR, 67037, Strasbourg Cedex 2, France*
[4] *Departament de Física de la Materia Condensata, Universitat de Barcelona - C. de Martí i Franquès 1, 08028 Barcelona, Spain*

received 20 December 2016; accepted in final form 27 February 2017
published online 13 March 2017

PACS 75.75.-c – Magnetic properties of nanostructures
PACS 75.50.Tt – Fine-particle systems; nanocrystalline materials
PACS 75.30.Gw – Magnetic anisotropy

Abstract – We present results on low-temperature magnetization approaching the saturation law in aligned bundles of CNTs with ferromagnetic nanoparticles embedded inside inner channels of nanotubes for two directions of the magnetic field, parallel and perpendicular to the CNT axes. Elaborating experimental data, we were able to extract the explicit form of the correlation functions describing the orientation of the magnetic anisotropy axes in real space. In the parallel field the long-range coherence in the magnetic anisotropy axes is the characteristic feature. In the perpendicular direction the peculiar feature is the 2D exchange coupling. The nature of the exchange interaction and the role of the CNT medium in it is also discussed.

Introduction. – A lot of research activity is devoted to the magnetic properties of ferromagnetic nanoparticles distributed inside a matrix material (magnetic nanocomposites). Increased coercivity, saturation magnetization M_s and magnetic anisotropy have been already reported for different kinds of magnetic nanocomposites [1–3]. In addition, cooperative effects between ferromagnetic nanoparticles (NPs) and matrix material could be of particular interest both from the fundamental and the practical point of view. Such kind of interaction is determined by many factors, like arrangement of NPs in the matrix, electrophysical and magnetic properties of the matrix material, as well as NP/matrix interfaces. These factors, in turn, depend on the technological method which is applied for the NPs embedding into the matrix. Different methods are currently used to fabricate matrix dispersed NPs. Among others it is worth mentioning co-precipitation, thermal decomposition, emulsion methods [4], co-evaporation [5], electrochemical processes [6] and chemical vapor deposition (CVD) [7]. The material of the matrix could also vary in a wide range, covering polymers [5], silica [4], porous silicon [8], carbon nanotubes (CNT) [6,9], etc.

From the viewpoint of cooperative effects, CNT-based magnetic nanocomposites are of special interest. Indeed, such material presents a porous conducting discontinuous medium. Ferromagnetic NPs can be localized inside or outside of the nanotube inner channels. The aspect ratio of inclusions can vary in a wide range, from 1 to approximately 100, indicating formation of objects with variable morphology, from nanoparticles to nanowires. The role of the CNT in the interparticle interaction is of great importance. In spite of porosity, the CNT matrix usually is a well-conducting object. Therefore, this conducting medium can provide indirect exchange coupling (IEC) between ferromagnetic nanoparticles [10,11] with long-range character [12,13]. Moreover, defective carbon allotropies, including graphene, which forms the CNT walls, are ferromagnetic materials even at room temperature [14–16]. Finally, properties of the ensemble of ferromagnetic NPs embedded in the CNT medium are well explained within the random anisotropy model (RAM) [17–19]. All this

is reflected in the particular interparticle interaction, creating peculiarities in the interplay between the exchange coupling and magnetic anisotropy [19,20], neglecting the magnetic dipole interaction, which is characteristic of a random anisotropy ferromagnet [21].

Usually the exchange coupling between crystalline NPs can be considered when the inequality $R_c < R_f$ is fulfilled. Here R_c is the average radius of the NP and R_f is the exchange correlation length. The peculiarity of the exchange correlations depends on the dimensionality of the NP arrangement d. In particular, for $H \ll H_{ex}$ (H_{ex} being the exchange field) phenomenological law of the approach to saturation (LAS) can be estimated as

$$\frac{\delta M}{M_s} = \frac{M(H) - M_s}{M_s} \sim H^{-\alpha}, \qquad (1)$$

where the exponent α is determined by the dimensionality d, $\alpha = \frac{4-d}{2}$ [17]. For example, for the three-dimensional (3D) case $\alpha = 1/2$, while for the two-dimensional (2D) interaction $\alpha = 1$. When $\alpha = 2$, it means that the magnetic anisotropy dominates. Usually this occurs at $H \gg H_{ex}$.

From eq. (1) it follows that the analysis of the magnetization curve $M(H)$ in the region where M approaches saturation could give, in a relatively simple way, useful information about the dimensionality of the NPs interaction which, in turn, could be related to their arrangement. Indeed, many experimental works have been dedicated to such kind of study. In particular, 3D dimensionality was unambiguously established in different amorphous compounds [22] and nanostructured Fe and Ni materials [23]. 2D dimensionality is a characteristic feature of thin films with thickness $d_f < R_f$ [24] and of nanocrystalline thick materials ($d_f \gg R_f$), but with anisotropic ferromagnetic correlation lengths, $R_f^{||} \gg R_f^{\perp}$ [25]. Finally, a 1D system of exchange-coupled ferromagnetic NPs was reported for Fe nanowires embedded inside inner channels of CNTs [26]. In all these studies authors usually demonstrated, as the evidence of particular dimensionality, the $\delta M/M_s$ *vs.* $H^{-\alpha}$ plot only for a single exponent α. The obtained agreement between the experimental data and eq. (1) with a single exponent α was used as the main argument, supporting a particular dimensionality.

Recently, it has been demonstrated that, at least for CNT-based magnetic nanocomposite, such approach does not provide an unambiguous answer about the real dimensionality [27]. Data were related to the parallel magnetic field with respect to the CNT axes. It was found that all possible exponents of eq. (1) may explain the experimental data up to a certain extent. The only thing that changes for different exponents, is the range of the magnetic field in which the law (1) is carried out.

Generally speaking, the magnetic-field range considered in ref. [27] is of the order of the exchange field, $H \sim H_{ex}$. It means that eq. (1) is no longer valid and a more general approach should be considered, in which the magnetic ordering is described by the correlation function of the magnetic anisotropy axes in real space, $C(r)$ [28]. This approach allows to obtain important information about the mechanism of magnetic interaction between NPs intercalated inside CNT: interplay between exchange coupling and magnetic anisotropy, role of the coherent anisotropy (CA) and its relation with the random anisotropy, and, finally, indication of the impact of the CNT medium on the interparticle interaction [27]. The expression for LAS in this case depends on the dimensionality of the system. For 2D the magnetization approaches saturation as [17]

$$\frac{\delta M}{M_s} = \frac{1}{32}\left(\frac{H_r}{H_{ex}}\right)^2 \left(\frac{H_{ex}}{H}\right)^{1/2} \times \int_0^\infty \mathrm{d}^3 x C(x) x^2 K_1\left[x\left(\frac{H}{H_{ex}}\right)^{1/2}\right], \qquad (2)$$

where H_r is the random anisotropy field, the coordinate x is normalized to the R_a value, the length over which the magnetic anisotropy axes are correlated and K_1 is the modified Hankel function.

For other dimensionalities, the general expression for LAS is [29]

$$\frac{\delta M}{M_s} = \frac{1}{30}\left(\frac{H_r}{H_{ex}}\right)^2 \left(\frac{H_{ex}}{H}\right)^{1/2} \times \int_0^\infty \mathrm{d}^3 x C(x) x^2 \exp\left[-x\left(\frac{H}{H_{ex}}\right)^{1/2}\right]. \qquad (3)$$

The analysis of the experimental data at $H \sim H_{ex}$ according to eqs. (2) and (3) can provide an explicit form of $C(x)$. Even the information about the orientational order could be extracted from $C(x)$ [30].

In this work, developing the approach proposed in ref. [27], we continued the study of the magnetization approaching saturation for CNT-based composite with low content of ferromagnetic NPs at two orientations of the magnetic field, parallel and perpendicular to the CNT axes. All analyzed data are for low temperature, $T = 2\,\mathrm{K}$. We demonstrate that both the CA and IEC via the CNT conducting medium could really contribute to the interparticle interaction in the parallel field. The contribution of the coherent magnetic anisotropy becomes negligibly small in the perpendicular field, at which the exchange coupling dominates. We demonstrate that the range of the IEC in our samples could propagate up to hundreds of nanometers due to the spin-orbit interaction.

Experimental. – Vertically aligned arrays with low content of ferromagnetic NPs have been synthesized by floating catalyst CVD at ambient pressure on Si/SiO_2 substrates [19]. Dissolved in xylene ferrocene $Fe(C_5H_5)_2$ was used as a source of catalytic particles. All technological parameters were kept constant except for the concentration of ferrocene C_F in the ferrocene/xylene solution. We synthesized samples with $C_F = 0.5, 0.6, 0.7$ and $0.8\,\mathrm{wt.\%}$ (samples 05, 06, 07 and 08, respectively).

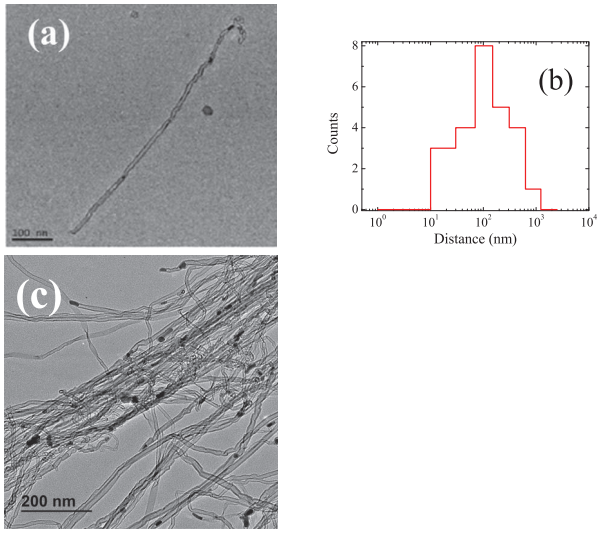

Fig. 1: (Colour online) (a) TEM image of a single CNT which was selected from the array synthesized with $C_F = 0.5$ wt.%. (b) Historgam of the distance distribution between adjacent NPs along one single nanotube. (c) TEM image of a CNT bundle synthesized with $C_F = 0.7$ wt.%.

Low ferrocene content provided the localization of the iron-based catalytic NPs mainly in the inner channels of CNT [27,31]. On the other hand, low C_F values allow the formation of defective nanotubes, which was ascertained by Raman spectroscopy [32]. As a result, we synthesized vertically aligned arrays of defective multiwall CNTs with typical thickness of ≈ 20 μm, average nanotube diameter $\varnothing_{CNT} \approx 20$–30 nm and the number of walls in one tube not exceeding 15. The diameter of embedded NPs was close to the $\varnothing_{CNT}$ inner values [27]. Nanoparticles are formed by cementite Fe_3C and are single crystalline. Both these facts were proved directly by the high-resolution TEM (HRTEM) study [27,32]. SEM investigations have shown that the average distance between the nanotubes is around 50 nm. In addition, an array of nanotubes has a clearly defined axis oriented perpendicular to the plane of the substrate, but the nanotube throughout its length can bend and intersect with other CNTs, creating bundles, see fig. 1 of ref. [27]. This leads to the formation of paths for current and the whole medium is conductive. More details about the CNT fabrication and characterization can be found elsewhere [9,19,20,27].

A distinctive feature of the studied samples is not only the location of the ferromagnetic NPs inside the nanotube inner channel, but also a large interparticle distance within a single nanotube. In fig. 1(a) we show the TEM image of a single CNT which was selected from the array of nanotubes synthesized with $C_F = 0.5$ wt.%. From fig. 1(a) it is clearly seen that the nanotube is almost empty, the embedded NPs are strongly distant from each other. In fig. 1(b) we show the result of the systematic TEM study of the distances between the adjacent NPs belonging to one CNT. We plot a histogram of the distribution of

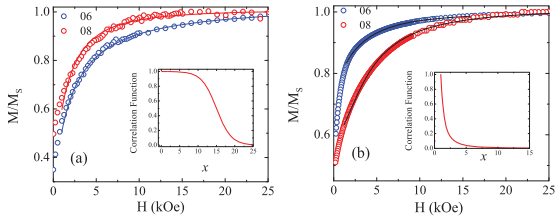

Fig. 2: (Colour online) Measured (symbols) and calculated (lines) $M(H)$ dependences of two samples, 06 and 08. $T = 2$ K. (a) Parallel magnetic field; (b) perpendicular magnetic field. Insets: correlation functions extracted from the fitting procedure. For details of the calculations see the text.

distances between the adjacent nanoparticles. This result shows that the most frequent distance between neighbor nanoparticles is close to 100 nm.

Now we would like to comment the presence of free NPs in fig. 1(a). We believe that the origin of particles outside CNT is either an impurity or is associated with a particular process of preparing the sample for TEM. To carry out this study, the grid has been prepared by a dry dispersion of CNT on a copper grid covered with a wholly amorphous membrane. It means that we mechanically destroy the oriented array of CNTs, put the obtained powder on the grid and then we tried to find the appropriate unbroken CNT, which was the subject of our study. During this process, some particles belonging to a huge number of destroyed CNTs may also be taken into the field of the microscope. In order to unambiguously assert the insertion of NPs only into CNTs in fig. 1(c) we show the TEM image of a CNT bundle of another sample, synthesized with $C_F = 0.7$ wt.%. It is clearly seen that for each of them at least one NP is embedded inside and no NPs are observed outside.

Magnetic measurements have been done at $T = 2$ K by using a commercial SQUID magnetometer with the applied field up to 80 kOe for both parallel and perpendicular orientations with respect to the CNT axes. The experimental data in the parallel field for sample 08 have been partially reported in ref. [27].

Results and discussion. – In fig. 2 we show the $M(H)$ curves measured for samples 06 and 08 in parallel (fig. 2(a)) and perpendicular (fig. 2(b)) fields. The analysis of the experimental data according to eq. (1) revealed that for parallel orientation the experimental data are better explained by the exponent $\alpha = 2$, in accordance with the result of [27]. On the other hand, for the *perpendicular* field the result changes drastically. We did not observe the noticeable linear part in the plot $\delta M(H^{-2})$. While the contributions of the $H^{-1/2}$ (3D) and H^{-1} (2D) terms were significant. These results are presented in figs. 3(a)–(c), in which we replot data of fig. 2(b) according to eq. (1) using exponents $\alpha = 2$, 1 and 1/2, respectively. In fig. 3(d) δM *vs.* H^{-2} is plotted for the samples 06 and 08 in the *parallel* magnetic field. Evidently, the law (1) with the exponent

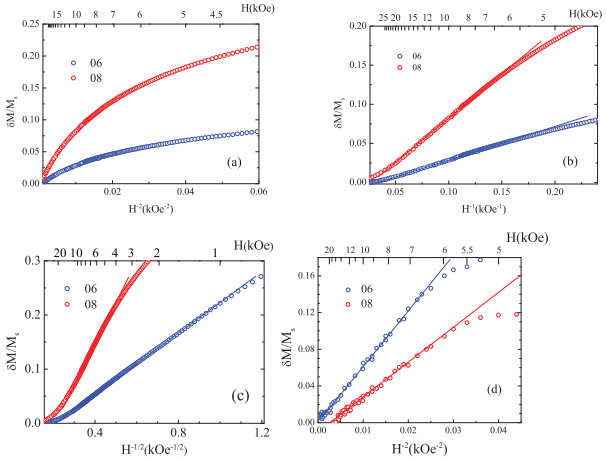

Fig. 3: (Colour online) Analysis of LAS according to eq. (1) for samples 06 and 08. $T = 2\,\mathrm{K}$. (a)–(c) Perpendicular magnetic field; (d) parallel magnetic field.

$\alpha = 2$ fits well the data. It should be noted that in the parallel field at low T data can be fitted also by exponents $\alpha = 1$ and $\alpha = 1/2$, as was demonstrated in [27]. The top axis in each plot represents the absolute values of the magnetic field. This result indicates that, while for parallel orientation, as was already demonstrated previously, the magnetic anisotropy is strong [19], in the perpendicular field there is not any significant feature of the anisotropy, thus the exchange interaction prevails.

To get deeper insight into the problem we applied the approach based on the correlation function. For that we start analyzing eqs. (2) and (3). As follows from eqs. (2) and (3), knowing the micromagnetic parameters H_r, H_{ex}, M_s, R_a and performing the inverse K-transform (Meijer transform) for eq. (2) and the inverse Laplace transform for eq. (3), it is possible to obtain the explicit form of the correlation function $C(r)$. In order to reduce the number of fitting parameters, we directly measured the saturation magnetization value M_s, and we assumed R_a to be equal to the radius of the nanoparticle [23]. In the articles [19,20,27] the estimations of the H_{ex} and H_r values for CNT nanocomposites studied in the present work have also been performed. Usually these values are of the order of a few kOe. This fact simplifies the fitting procedure. Also, based on the result of ref. [27] we introduced the CA into the considerations. As was proposed in [33], when the CA axis is aligned along the direction of the external magnetic field, its contribution can be taken into account substituting the external field H by $H + H_{ca}$ (H_{ca} being the CA field). Thus, we can rewrite eq. (2) in a form more convenient for the experimental data elaboration,

$$\frac{\beta}{p^2} = \left[\left(\frac{H_r}{H_{ex}}\right)^2 \frac{4\pi}{32p^{3/2}} \int_0^\infty \mathrm{d}x C(x) x^{3/2} \sqrt{px} K_1(px)\right], \tag{4}$$

where $p = (H/H_{ex})^{1/2}$ and β is a constant, which is determined by the slope of the dependence (1).

The correlation function in the 2D case is obtained applying the K-transform, $F_{2D}(p) = \int_0^\infty \mathrm{d}x f(x) \sqrt{px} K_1(px)$ [34]. For other dimensionalities we tried to fit the experimental data by applying eq. (3). For that it is necessary to estimate the Laplace integral $F_{3D}(p) = 4\pi \int_0^\infty \mathrm{d}x \exp(-px) x^2 C(x)$.

As a result of the fitting procedure, for the perpendicular field in the 2D case the experimental data are well fitted using the following correlation function:

$$C_{2D}(x) = \frac{1}{x^2} \frac{1}{(x^2 - a^2)^{1/2}} \left[\left[x + (x^2 - a^2)^{1/2}\right]^{2m} + \left[x - (x^2 - a^2)^{1/2}\right]^{2m}\right], \quad x > a \tag{5}$$

with constants $a = 0.01$ and $m = 0.07$.

In the 3D case the correlation function was obtained in [27],

$$C_{3D}(x) = b^{-1/2} x^{(\nu/2)-2} J_\nu \left[2b^{1/2} (x + x_0)^{1/2}\right], \tag{6}$$

where J_ν is the ν-th order Bessel function of the first kind, b and x_0 are constants.

In the case in which the contribution of the anisotropy is significant, the correlation function is [27]

$$C_a(x) = \frac{1}{1 + \exp\left(\frac{x - x_{1/2}}{2}\right)}, \tag{7}$$

where $x_{1/2}$ is a coordinate at which the amplitude of the correlation function reduces to 1/2.

The fitting procedure of the $M(H)$ data in parallel and perpendicular magnetic fields revealed that for the parallel field the correlation function $C_a(x)$ explains better the experimental data, see lines in fig. 2(a). In addition, the term of the CA is of great importance. Curves in fig. 2(a) are plotted with the following parameters: $H_{ex} = 4$ kOe for both samples, $H_r = 3.8(3.2)$ kOe and $H_{ca} = 2.0(3.6)$ kOe for sample 06 (08). Note, that, in agreement with the previously reported result [27], without H_{ca} it was impossible to fit the data. The correlation function of the sample 08 is plotted in the inset to fig. 2(a). Correlations propagate up to $x_{1/2} \approx 15$, which corresponds to $r_{1/2} \approx 150$–200 nm. These values are very close to the mean distance between adjacent NPs embedded in one CNT, see fig. 1(b). Such long-range correlations manifest the crucial role of the coherence anisotropy in the determination of the magnetic properties of CNT-based nanocomposite in the parallel field [19]. It should be underlined that the $M(H)$ data in the parallel field can also be fitted applying the correlation function $C_{3D}(x)$ (not shown here), in accordance with the fact that the exponent α of the phenomenological LAS (1) can be equal to 1/2. The agreement in this case between the experimental data and theory is not so good as for $C_a(x)$, but the term H_{ca} is still important. As a matter of fact, without it, the data cannot be fitted at all. Nevertheless, this fact underlines the extremely complex nature of the interparticle interaction via the CNT

medium. The alignment of the CNTs also plays a crucial role in the observed long-range correlations in the parallel field. When the alignment is destroyed, *i.e.*, the oriented array of CNTs becomes a powder, the exponent α in LAS (1) is no longer equal to 2, and becomes equal to 1/2 [20].

In the perpendicular field the result is different from what was observed in parallel. The correlation function $C_{2D}(x)$ describes the $M(H)$ data better. This result is shown in fig. 2(b) by the solid lines. The parameters of the fit are $H_{ex} = 4$ kOe for both samples and $H_r = 2.3$ and 3.7 kOe for samples 06 and 08, respectively. We found no necessity of taking into account the term of the CA during the fitting procedure in the perpendicular field, *i.e.*, $H_{ca} = 0$ for both samples. The obtained correlation function $C_{2D}(x)$ for sample 08 is shown in the inset to fig. 2(b). In this case correlations propagate up to $r_{1/2} \approx 15$–20 nm, *i.e.*, the size of the ferromagnetic NP, as it should be in the RAM [17].

The obtained strong dependence of the correlation order of the magnetic anisotropy axes on the direction of the applied magnetic field underlines the impact of the CNT medium on the mechanism of the interparticle interaction. In fact, as we already mentioned above, NPs are embedded inside inner channels of CNTs. The presence of a preferred direction in the orientation of the nanotubes leads to a vertical arrangement of the nanoparticles. In this sense, in the parallel field the arrangement of NPs is ordered. They aligned along a unique axis which coincides with the axis of CNT. As our results demonstrate, this axis also coincides with the direction of the coherence anisotropy of each NP. This leads to a macroscopically large correlation order, hundreds of nanometers, which coincides with the mean interparticle distance. For the perpendicular orientation of the magnetic field the average projection of the coherent anisotropy axes is negligibly small. Therefore, the fitting procedure in this case was successful without considering the H_{ca} term. The obtained 2D character of the interparticle interaction in the perpendicular direction also could be explained involving the CNT medium and particular arrangement of NPs. Indeed, in the vertical direction the mean distance between NPs is close to 100–150 nm, see fig. 1. On the other hand, as was established previously [19,27], the average distance between nanotubes does not exceed 50 nm. It means that in the direction perpendicular to the CNT axes NPs are packed more densely than in the parallel one. This could be the reason for the 2D behavior in the perpendicular field.

The unclear question which still remains is the origin of the exchange interaction between the NPs, distant from each other over tens or even hundreds of nanometers. Actually, the usual random anisotropy model cannot answer this question. We believe that, again the particular properties of the CNT medium are responsible for the origin of the abnormal exchange interaction. The peculiarity of the CNT-based nanocomposite is the conductivity of the CNT matrix. Therefore, it is naturally to suppose that the IEC via the conducting electrons is the origin of the exchange interaction between distant NPs. In ref. [13] the Rudermann-Kittel-Kasuya-Yosida (RKKY) interaction in single-walled semiconductor CNT with diameters of the order of 1 nm was considered. It was demonstrated that, due to the spin-orbit interaction (SOI) [35] the IEC along the CNT axis could reach the value of 1 micrometer [13]. For such a large length of the IEC the constant of spin-orbit splitting equal to 6 meV and the Fermi level shift $\mu \sim 0.5$ eV are required [13,36]. This significant shift of the Fermi level can be induced by any defects of the nanotubes or their doping [37,38]. The large spin-orbit coupling was experimentally detected in CNTs [39]. We believe, that our defective conducting nanotubes could be a suitable environment for the indirect exchange interaction.

Based on the model developed by Klinovaja and Loss [13] we looked for the indications of the possibility of the long-range RKKY interaction in our samples. A theoretical model is based on the consideration of the properties of single-walled CNT (SWNT). The diameter of SWNT does not exceed few nanometers. Strictly speaking, our nanotubes do not fit the criterion of single-walled. However, we can assume with a very effective probability that the indirect exchange coupling occurs through one shell that could be the internal shell. Therefore, we considered for simplicity that the ferromagnetic NP is in contact only with the inner shell of CNT and the coupling propagates along this one inner shell. The conductivity of this shell in defective MWCNTs, as was demonstrated experimentally, could be significant and comparable to the conductivity of the outermost shell [40,41]. The diameter of the inner shell determines the diameter of the NP and in our calculations was selected as $\varnothing_{CNT} = 25$ nm. The axis z is oriented along the CNT axis. To analyze the decay of the RKKY interaction in the presence of SOI the low-frequency component of the oscillations of the normalized spin susceptibility χ along the CNT axis was examined,

$$\chi(z) = \mathrm{si}(2k_+|z|)/2 \pm \mathrm{si}(2k_-|z|), \tag{8}$$

where $\mathrm{si}(y) = \int_0^y \frac{\sin t}{t}\mathrm{d}t - \frac{\pi}{2}$. The effective wave vectors k_+ and k_- are defined within the model [13] and depend on the diameter of the CNT, its chirality, parameters of the SOI and μ. For certain combinations of these parameters the exchange coupling is long-range and propagates over hundreds of nanometers [13].

Following this scenario, we calculated the spin susceptibility looking for a value of the shift of the Fermi level μ due to SOI, which would lead to the decay length of the order of hundreds of nanometers. It should be noted that μ was the only completely free adjustable parameter. The obtained result is presented in fig. 4, in which we plot the amplitude envelope of the spin susceptibility oscillations along the z-axis for $\mu = 25$ meV. Other parameters used in these calculations are as follows. Chiral indices were chosen as (235,129). These values correspond to the $\varnothing_{CNT} = 25$ nm. The angle of chirality in this case is equal to 39.54° and the circumferential direction

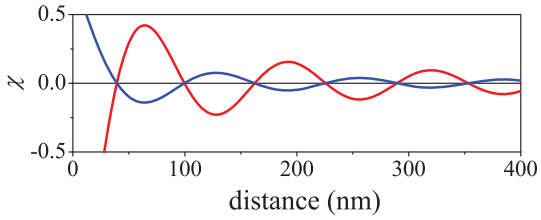

Fig. 4: (Colour online) Decay of the spin susceptibility amplitude oscillations along the CNT axis. Blue and red lines correspond to the envelope of the spin susceptibility oscillations, whose period is of the order of 0.5 nm. For details of the calculations see the text.

$k_G = 0.053\,\mathrm{nm}^{-1}$. The constant of spin-orbit splitting Δ_{SO} following data of other authors, was chosen to be equal to 6 meV [13,36]. Finally, the period of oscillations of spin susceptibility for this set of parameters is of the order of 0.5 nm, so they are not shown in fig. 4.

The obtained chiral indices emphasize the fact that the curvature effects are rather negligible, as should be in a purely theoretical case for a SWCNT of such large diameter. It follows from the result of fig. 4 that for the considered parameters of the nanotube the IEC could propagate on hundreds of nanometers. Even if this result can be regarded only as an indication that the long-range interaction can really occur in our samples, it strongly supports the idea that the IEC directly affects the coupling between ferromagnetic NPs via the CNT medium as was clearly derived from the elaboration of the $M(H)$ data. To make this statement more solid, it is necessary to carry out the calculations for multi-walled CNT. In addition, the external magnetic field strengthens the SOI and, consequently, could intensify the exchange coupling at large distances.

In summary, the analysis of the LAS for the oriented arrays of MWCNTs with ferromagnetic NPs embedded inside carbon nanotubes has been performed. The magnetic field was applied both parallelly and perpendicularly to the CNT axis. For the parallel orientation the magnetic anisotropy is of great importance. It is caused by the existence of the coherence anisotropy. In the perpendicular direction the exchange coupling dominates and the contribution of the coherence anisotropy is negligibly small. Moreover, the exchange interaction is of 2D type. Fitting the $M(H)$ data, we obtained the correlation function of the magnetic anisotropy axes in the 2D case. The magnetic coupling between NPs distant from each other for tens and hundreds of nanometers could occur via the RKKY interaction. Calculations of the amplitude of spin susceptibility and its decay along the CNT axis confirm this hypothesis. The obtained results suggest that aligned arrays of CNTs with embedded ferromagnetic NPs are potentially useful for magnetoelectronics and spintronics.

* * *

Authors acknowledge O. Ersen and G. Melinte from ICPMS, Strasbourg, France for TEM analysis of the sample synthesized with $C_F = 0.5$ wt.% and J. Ghanbaja from Institute of Jean Lamour, Nancy, France for TEM analysis of the sample synthesized with $C_F = 0.7$ wt.%.

REFERENCES

[1] Dormann J. L., Fiorani D. and Tronc E., *Adv. Chem. Phys.*, **98** (1997) 283.
[2] Gubin S. P., Koksharov Y. A., Khomutov G. B. and Yurkov G. Yu., *Russ. Chem. Rev.*, **74** (2005) 489.
[3] Proctor T. C., Chudnovsky E. M. and Garanin D. A., *J. Magn. & Magn. Mater.*, **384** (2015) 181.
[4] Liu J., Qiao S. Z., Hu Q. H. and Lu G. Q. (Max), *Small*, **7** (2011) 425.
[5] Faupel F., Zaporojtchenko V., Strunkus T. and Elbahri M., *Adv. Eng. Mater.*, **21** (2010) 1177.
[6] Wildgoose J. J., Banks C. E. and Compton R. G., *Small*, **2** (2006) 182.
[7] Jourdain V. and Bichara C., *Carbon*, **58** (2013) 2.
[8] Dolgiy A. L., Redko S. V., Komissarov I., Bondarenko V. P., Yanushkevich K. I. and Prischepa S. L., *Thin Solid Films*, **543** (2013) 133.
[9] Labunov V. A., Danilyuk A. L., Prudnikava A. L., Komissarov I., Shulitski B. G., Speisser C., Antoni F., Le Normand F. and Prischepa S. L., *J. Appl. Phys.*, **112** (2012) 024302.
[10] Costa Jr., A. T., Kirwan D. F. and Ferreira M. S., *Phys. Rev. B*, **72** (2005) 085402.
[11] He J., Zhou P., Ma S. Y., Zhang K. W. and Sun L. Z., *Sci. Rep.*, **4** (2014) 4014.
[12] Costa A. T., Rocha C. G. and Ferreira M. S., *Phys. Rev. B*, **76** (2007) 085401.
[13] Klinovaja J. and Loss D., *Phys. Rev. B*, **87** (2013) 045422.
[14] Esquinazi P. and Höhne R., *J. Magn. & Magn. Mater.*, **290-291** (2005) 20.
[15] Yazev O. V., *Rep. Prog. Phys.*, **73** (2010) 056501.
[16] Giesbers A. J. M., Uhlirová K., Konečny M., Peters E. C., Burghard M., Aarts J. and Flipse C. F. J., *Phys. Rev. Lett.*, **111** (2013) 166101.
[17] Chudnovsky Eugene M., in *The Magnetism of Amorphous Metals and Alloys*, edited by Fernandez-Baca J. A. and Ching Wai-Yim (World Scientific, Singapore) 1995, Chapt. 3, pp. 143–175.
[18] Komogortsev S. V., Iskhakov R. S., Balaev A. D., Kudashov A. G., Okotrub A. V. and Smirnov S. I., *Phys. Solid State*, **49** (2007) 734.
[19] Danilyuk A. L., Prudnikava A. L., Komissarov I. V., Yanushkevich K. I., Derory A., Le Normand F., Labunov V. A. and Prischepa S. L., *Carbon*, **68** (2014) 337.
[20] Prischepa S. L., Danilyuk A. L., Prudnikava A. L., Komissarov I. V., Labunov V. A. and Le Normand F., *Phys. Status Solidi C*, **11** (2014) 1074.
[21] Imry Y. and Ma S.-K., *Phys. Rev. Lett.*, **35** (1975) 1399.
[22] Chudnovsky E. M., *J. Appl. Phys.*, **64** (1988) 5770.
[23] Löffler J. F., Meier J. P., Doudin B., Ansermet J.-P. and Wagner W., *Phys. Rev. B*, **57** (1998) 2915.
[24] Chudnovsky E. M., *J. Magn. & Magn. Mater.*, **40** (1983) 21.
[25] Iskhakov R. S., Komogortsev S. V., Balaev A. D. and Gavriliuk A. A., *J. Magn. & Magn. Mater.*, **374** (2015) 423.

[26] Iskhakov R. S., Komogortsev S. V., Balaev A. D., Okotrub A. V., Kudashov A. G., Kuznetsov V. I. and Butenko Yu. V., *JETP Lett.*, **78** (2003) 236.
[27] Danilyuk A. L., Komissarov I. V., Labunov V. A., Le Normand F., Derory A., Hernandez J. M., Tejada J. and Prischepa S. L., *New J. Phys.*, **17** (2015) 023073.
[28] Chudnovsky E. M. and Serota R. A., *J. Phys.: Solid State Phys.*, **16** (1983) 4181.
[29] Chudnovsky E. M., *J. Magn. & Magn. Mater.*, **79** (1989) 127.
[30] Chudnovsky E. M. and Tejada J., *Europhys. Lett.*, **23** (1993) 517.
[31] Blank V. D., Gorlova I. D., Hutchison J. L., Kiselev N. A., Ormont A. B., Polyakov E. V., Sloan J., Zakharov D. N. and Zybtsev S. G., *Carbon*, **38** (2000) 1217.
[32] Prischepa S. L., Danilyuk A. L., Prudnikava E. L., Komissarov I. V., Labunov V. A., Yanushkevich K. I. and Le Normand F., *in Nanomagnetism*, edited by Gonzalez Estevez J. M. (One Central Press, Manchester) 2014, Chapt. 9, pp. 227–245.
[33] Chudnovsky E. M., Saslow W. M. and Serota R. A., *Phys. Rev. B*, **33** (1986) 251.
[34] Erdélyi A. (Editor), *Tables of Integral Transforms*, Vol. **2** (McGraw-Hill Book Co., New York) 1954.
[35] Klinovaja J., Schmidt M. J., Braunecker B. and Loss D., *Phys. Rev. Lett.*, **106** (2011) 156809.
[36] Min H., Hill J. E., Sinitsyn N. A., Sahu B. R., Kleinman L. and MacDonald A. H., *Phys. Rev. B*, **74** (2006) 165310.
[37] Zhou W., Vavro J., Nemes N. M., Fischer J. E., Borondics F., Kamarás K. and Tanner D. B., *Phys. Rev. B*, **71** (2005) 205423.
[38] Kim S., Jo I., Dillen D. S., Ferre D. A., Fallahazad B., Yao Z., Banerjee S. K. and Tutuc E., *Phys. Rev. Lett.*, **108** (2012) 116404.
[39] Steele G. A., Pei F., Laird E. A., Jol J. M., Meerwaldt H. B. and Kouwenhoven L. P., *Nat. Commun.*, **4** (2013) 1573.
[40] Collins P. G., Arnold M. S. and Avouris P., *Science*, **292** (2001) 706.
[41] Stetter A., Vancea J. and Back C. H., *Appl. Phys. Lett.*, **93** (2008) 172103.